

Subpercent constraints on the cosmological temperature evolutionA. Avgoustidis,^{1,*} R. T. Génova-Santos,^{2,3,†} G. Luzzi,^{4,‡} and C. J. A. P. Martins^{5,6,§}¹*School of Physics and Astronomy, University of Nottingham, University Park, Nottingham NG7 2RD, England*²*Instituto de Astrofísica de Canarias, C/Vía Láctea s/n, La Laguna, Tenerife, Spain*³*Departamento de Astrofísica, Universidad de La Laguna (ULL), 38206 La Laguna, Tenerife 38200, Spain*⁴*Department of Physics, Sapienza, University of Rome, Piazzale Aldo Moro 2, I-00185 Rome, Italy*⁵*Centro de Astrofísica, Universidade do Porto, Rua das Estrelas, 4150-762 Porto, Portugal*⁶*Instituto de Astrofísica e Ciências do Espaço, CAUP, Rua das Estrelas, 4150-762 Porto, Portugal*
(Received 20 November 2015; published 12 February 2016)

The redshift dependence of the cosmic microwave background temperature is one of the key cosmological observables. In the standard cosmological model, one has $T(z) = T_0(1+z)$, where T_0 is the present-day temperature. Deviations from this behavior would imply the presence of new physics. Here we discuss how the combination of all currently available direct and indirect measurements of $T(z)$ constrains the common phenomenological parametrization $T(z) = T_0(1+z)^{1-\beta}$ and obtain the first subpercent constraint on the temperature growth index $1-\beta$. Specifically, we find $\beta = (7.6 \pm 8.0) \times 10^{-3}$ at the 68.3% confidence level.

DOI: [10.1103/PhysRevD.93.043521](https://doi.org/10.1103/PhysRevD.93.043521)**I. INTRODUCTION**

Over the last three decades cosmology has been transformed from a purely theoretical into an observational discipline. This has been possible thanks to a plethora of different observables, notably the cosmic microwave background (CMB) anisotropies at $z \approx 1100$ [1], the baryon acoustic oscillations (BAO) seen in the distribution of galaxies at $z \approx 0.5$ [2] or the type Ia supernovae which demonstrated the accelerated expansion of the Universe [3,4]. These have led to the consolidation of the so-called Λ CDM “concordance model,” according to which the Universe is homogeneous on large scales, has a nearly flat geometry, is currently undergoing accelerated expansion, and is made of dark energy (68%), cold dark matter (27%), and ordinary matter (5%).

Despite the extraordinary success of finding completely independent observables converging into a common theoretical framework, there are still aspects that are not fully understood or well characterized. Probably the most striking one is that 95% of the content of the Universe has not, so far, been experimentally detected in the laboratory (but has only been detected “mathematically”); this is in the form of dark energy and dark matter. This fact strongly hints at the existence of new physics beyond the standard Λ CDM model. In this context, it is important to explore laboratory or astrophysical probes that may provide evidence for the presence of this, still unknown, physics. In the present paper, we focus on testing the redshift dependence

of the CMB temperature, which is one of the core predictions of standard big bang cosmology that may be violated under nonstandard scenarios [5].

According to the big bang model, the CMB temperature evolves with redshift z as $T_{\text{CMB}}(z) = T_0(1+z)$, under the assumptions of adiabatic expansion and photon number conservation. There are, however, many nonstandard scenarios where these assumptions are not met (we will point out examples of them later) causing potentially observable deviations from the standard scaling. Therefore, direct or indirect measurements of the temperature-redshift relation provide constraints on scenarios beyond the standard Λ CDM paradigm. As will be discussed in Sec. II, there are several ways of obtaining direct constraints on $T(z)$, and these can be combined with indirect constraints coming from measurements of the so-called distance duality relation, presented in Sec. III. In the future, further indirect constraints will become available, for example from CMB spectral distortions [6]. In Sec. IV, we present joint constraints after combining the direct and indirect measurements of Secs. II and III. This updates the previous results of [5] and improves them by almost a factor of two, reaching for the first time subpercent precision on the temperature-redshift relation down to redshifts of $z \sim 3$. Finally, in Sec. V, we present the main conclusions derived from this study.

II. DIRECT CONSTRAINTS FROM CMB-TEMPERATURE MEASUREMENTS

Deviations of the standard CMB temperature scaling with redshift are usually described using the parametrization proposed by [7],

* Anastasios.Avgoustidis@nottingham.ac.uk

† rgs@iac.es

‡ gemma.luzzi@roma1.infn.it

§ Carlos.Martins@astro.up.pt

TABLE I. Measurements of the CMB taken from the literature, derived from the SZ effect towards galaxy clusters, and from CMB-photon induced rotational excitation of CO, C I, and C II in quasar spectral lines. N is the number of objects that were used and is different from unity only in cases of combining SZ observations towards many galaxy clusters. In those cases, we indicate the range of redshifts of the clusters. The fifth column shows the derived CMB temperature, and the last column the derived constraints on the β parameter describing the CMB-temperature redshift evolution. For all the measurements derived from SZ studies we show the β values which have been taken directly from the corresponding references and also the β values we have recalculated after removing the overlapping clusters among the various samples. In particular, in the case of Luzzi *et al.* (2015), we quote the final β constraint using their full sample of $N = 103$ clusters and also our recalculation after removing the four clusters ($N = 99$) in common with Saro *et al.* (2014), and after keeping all clusters with $z > 0.3$ and removing the only cluster in common with Saro *et al.* (2014) in that redshift range ($N = 33$). In the case of Luzzi *et al.* (2009), we quote the final β constraint using their sample of $N = 13$ clusters and also our recalculation after removing the six clusters ($N = 7$) in common with Luzzi *et al.* (2015) [e], and after keeping only clusters with $z > 0.3$ ($N = 2$). While Hurier *et al.* (2014) give a β constraint using their full cluster sample between $z = 0$ and $z = 1$, here we estimate β using only their $T_{\text{CMB}}(z)$ values between $z = 0.3$ and $z = 1$, in such a way that this constraint can be complemented with the one from de Martino *et al.* (2015). The same reanalysis has been applied to the Saro *et al.* (2014) sample. We have also estimated the β constraint using several $T_{\text{CMB}}(z)$ measurements in quasar spectral lines.

| Method | Reference | z | N | T_{CMB} (K) | β | Label | |
|----------------------------|--------------------------------------|----------------------------------|-----------|------------------------------|--------------------|--------------------|-----|
| | Saro <i>et al.</i> (2014) [18] | 0.055–1.350 | 158 | ... | 0.017 ± 0.030 | [a] | |
| | | 0.3–1.350 | | ... | 0.016 ± 0.031 | [b] | |
| | de Martino <i>et al.</i> (2015) [15] | < 0.3 | 481 | ... | -0.007 ± 0.013 | [c] | |
| | | 0.011–0.972 | 103 | ... | 0.012 ± 0.016 | [d] | |
| | Luzzi <i>et al.</i> (2015) [16] | 0.011–0.972 | 99 | ... | 0.014 ± 0.016 | [e] | |
| | | 0.3–0.972 | 33 | ... | 0.020 ± 0.017 | [f] | |
| | | 0.023–0.546 | 13 | ... | 0.065 ± 0.080 | [g] | |
| | Luzzi <i>et al.</i> (2009) [14] | 0.200–0.546 | 7 | ... | 0.044 ± 0.087 | [h] | |
| | | 0.3–0.546 | 2 | ... | 0.05 ± 0.14 | [i] | |
| | | 0–1 | 813 | ... | 0.009 ± 0.017 | [j] | |
| SZ effect towards clusters | | 0.30–0.35 | 81 | 3.562 ± 0.050 | | | |
| | | 0.35–0.40 | 50 | 3.717 ± 0.063 | | | |
| | | 0.40–0.45 | 45 | 3.971 ± 0.071 | | | |
| | | 0.45–0.50 | 26 | 3.943 ± 0.112 | | | |
| | | 0.50–0.55 | 20 | 4.380 ± 0.119 | | | |
| | | Hurier <i>et al.</i> (2014) [17] | 0.55–0.60 | 18 | 4.075 ± 0.156 | -0.006 ± 0.022 | [k] |
| | | | 0.60–0.65 | 12 | 4.404 ± 0.194 | | |
| | | | 0.65–0.70 | 6 | 4.779 ± 0.278 | | |
| | | | 0.70–0.75 | 5 | 4.933 ± 0.371 | | |
| | | | 0.75–0.80 | 2 | 4.515 ± 0.621 | | |
| | | 0.85–0.90 | 1 | 5.356 ± 0.617 | | | |
| | | 0.95–1.00 | 1 | 5.813 ± 1.025 | | | |
| | Muller <i>et al.</i> (2013) [19] | 0.89 | 1 | $5.0791^{+0.0993}_{-0.0994}$ | | | |
| | | 1.7293 | 1 | $7.5^{+1.6}_{-1.2}$ | | | |
| | Noterdeame <i>et al.</i> (2011) [20] | 1.7738 | 1 | $7.8^{+0.7}_{-0.6}$ | | | |
| | | 2.0377 | 1 | $8.6^{+1.1}_{-1.0}$ | | | |
| QSO absorption lines | Cui <i>et al.</i> (2005) [21] | 1.77654 | 1 | 7.2 ± 0.8 | 0.005 ± 0.022 | [l] | |
| | Ge <i>et al.</i> (2001) [22] | 1.9731 | 1 | 7.9 ± 1.0 | | | |
| | Srianand <i>et al.</i> (2000) [23] | 2.33771 | 1 | 6–14 | | | |
| | Srianand (2008) [24] | 2.4184 | 1 | 9.15 ± 0.72 | | | |
| | Noterdeame <i>et al.</i> (2010) [25] | 2.6896 | 1 | $10.5^{+0.8}_{-0.6}$ | | | |
| | Molaro <i>et al.</i> (2002) [26] | 3.025 | 1 | $12.1^{+1.7}_{-3.2}$ | | | |

$$T_{\text{CMB}}(z) = T_0(1+z)^{1-\beta}, \quad (1)$$

where β is a constant parameter ($\beta = 0$ in the standard scenario). The COBE-FIRAS experiment observations provided the most precise blackbody spectrum ever measured, with a temperature at the present epoch, $z = 0$, of $T_0 = 2.7260 \pm 0.0013$ K [8]. At higher redshifts, there are

presently two main methods used to obtain direct estimates of T_{CMB} , and from which constraints on β can be derived. The first method we will use was proposed nearly 40 years ago [9,10] and is based on multifrequency observations of the Sunyaev-Zel'dovich (SZ) effect [11], a distortion of the CMB spectrum produced towards galaxy clusters. As pointed out by [12], the existing large galaxy cluster

TABLE II. Joint constraints on the β parameter, derived through the combination of different constraints shown in Table I. The first column indicates the specific combination, represented by the labels listed in the last column of Table I. Individual and joint probably density functions are also plotted in Fig. 1.

| Combination | β |
|-------------------------------|-----------------------|
| $[b] + [c] + [f] + [i] + [l]$ | 0.0046 ± 0.0089^a |
| $[a] + [e] + [h] + [l]$ | 0.012 ± 0.012 |
| $[a] + [j] + [l]$ | 0.009 ± 0.012^b |
| $[c] + [k] + [l]$ | -0.004 ± 0.010 |

^aApplying the prescription of [29], we get 0.0064 ± 0.0086 .

^bIn this case, there are 16 overlapping clusters between the SPT sample from [18] and the Planck sample from [17]. If we use the value given in [18], in which they removed the 16 SPT clusters that were part of the main sample analyzed by Hurier *et al.* (2014), we have $\beta = 0.005 \pm 0.012$. However, in this last case, there are 13 overlapping clusters between [17] and [14].

catalogues together with very precise CMB data should allow precisions on β of the order of 0.01, a notable improvement with respect to initial constrains using a few clusters [13,14]. Recent results based on data from the Planck satellite [15–17] and from the *South Pole Telescope* [18] are shown in Table I. The most precise determinations are those from [15] and [16], and were obtained using, respectively, 481 and 103 galaxy clusters.

In order to combine different measurements, we have to ensure that they are independent, and therefore we have to remove any overlapping clusters. The analysis of [15] uses an unpublished catalogue containing clusters at $z < 0.3$, so to combine with their measurement we will remove all clusters in this redshift range from the other samples. In Table I, we show the β values resulting from the Luzzi *et al.* [16] subsamples containing

- (i) 99 clusters after removing the 4 clusters that are in common with the SPT sample in their full redshift range and
- (ii) 33 clusters at $z > 0.3$ after removing one cluster in common with the SPT sample.

We have the original posterior distributions of $T_{\text{CMB}}(z)$ for each of the clusters of [16], which have been used in this reanalysis. Similarly, [17] obtained $\beta = 0.009 \pm 0.017$ using 813 clusters out to $z \approx 1$. In Table I, we show the constraint we have derived using only their clusters at $z > 0.3$. To this end, we have used their $T_{\text{CMB}}(z)$ values obtained after stacking clusters in $\Delta z = 0.05$ redshift bins, and assuming Gaussian distributions. We also show the result of our reanalysis of the Saro *et al.* [18] sample using only their $z > 0.3$ clusters.

Estimations of $T_{\text{CMB}}(z)$ through the SZ effect are currently limited to $z \lesssim 1$ due to the scarcity of galaxy clusters at high redshifts. Estimates at $z > 1$ can be obtained through the study of quasar absorption line spectra which show energy levels that have been excited through atomic or molecular transitions after the absorption of

CMB photons [27]. If the relative populations of the different energy levels are in radiative equilibrium with the CMB radiation, then the excitation temperature gives the temperature of the CMB at that redshift. Early estimates based on this method must be regarded as upper limits on $T_{\text{CMB}}(z)$, since there could be significant contributions from other local sources of excitation. The first constraints using this method were only obtained 15 years ago [23], taking advantage of the enormous progress in high-resolution astrophysical spectroscopy; they use transitions in the UV range due to the excitation of fine-structure levels of atomic species like C I or C II [21–23,26]. More recently, improved constraints have been obtained from precise measurements of CO transitions and radio-mm transitions produced by the rotational excitation of molecules with permanent dipole moment [19,20,24,25]. In Table I, we show all these $T_{\text{CMB}}(z)$ estimates and our derived joint constraint $\beta = 0.005 \pm 0.022$.

It must be noted that recently the Planck Collaboration [1] obtained a very stringent constraint of $\beta = 0.0004 \pm 0.0011$ by combining CMB with large-scale structure data, after fixing the recombination redshift at $z_{\star} = 1100$. The very low error bar on β is due to the long lever-arm in redshift afforded by the CMB. However, that constraint only applies to models where the deviation from adiabatic evolution starts at the last scattering surface and, perhaps more importantly, the parametrization used, while adequate for low redshifts is not realistic for $z \sim 1100$. We leave the discussion of physically motivated high-redshift parametrizations for subsequent work.

Here we derive stringent constraints by combining the SZ and QSO absorption measurements shown in Table I. These two techniques complement each other not only because they cover different redshift ranges but also because they are subject to different types of systematics. Despite the shortage of targets, spectroscopic observations cover redshifts out to $z \approx 3$, therefore providing a longer lever-arm, as opposed to SZ observations that are restricted to $z < 1$ but benefit from a larger number of targets provided by the SZ cluster catalogues recently published [28].

In Table II, we present different possible combinations avoiding overlapping clusters, and the resulting joint constraints on β , which have been obtained by a standard inverse-variance weighted mean combination. In Fig. 1, the blue dashed lines represent the probability density functions (PDFs), assumed to be Gaussian, corresponding to different combinations presented in Table I. The solid blue lines represent the joint PDFs, which are just the multiplication of the individual PDFs. Due to a marginal disagreement among the data combined in case $[b] + [c] + [f] + [i] + [l]$, we have also applied the formula for a “skeptical” combination of experimental results, proposed by D’Agostini [29]. This PDF is represented by the magenta line in the top-left panel of Fig. 1. As soon as the individual results start to disagree, the combined distribution gets broader with respect to the

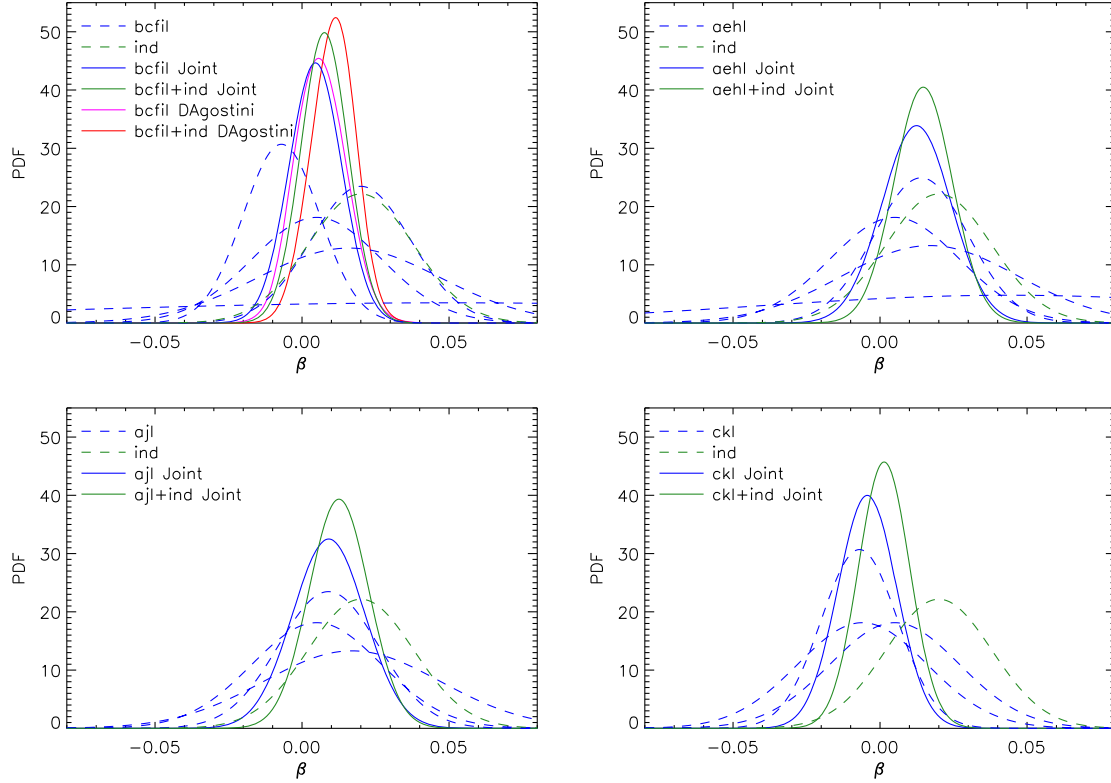


FIG. 1. Individual and joint probability density functions for each of the four combinations indicated in Tables II and III. Blue dashed lines show the individual PDFs derived from the different direct constraints on the β parameter shown in Table I, assuming Gaussian error distributions. The green dashed lines correspond to the indirect constraint derived in Sec. III. The solid blue lines show the joint constraints from direct measurements, from which the expected values and confidence intervals of Table II have been derived. The green solid lines correspond to the combination of direct and indirect constraints and are associated to the values of Table III. Finally, the magenta and red lines represent also a joint constraint, but obtained using the prescription of [29].

standard (weighted mean) result. However, if the agreement among individual results is good the combined distribution becomes narrower than the standard result. In this case, we find that the expected value is slightly shifted from the one obtained by the simple weighted mean. The intent of using this formula is to take into account the dispersion of the measurements, nevertheless this method returns lower errors. This is due to the fact that four of five measurements are in mutual agreement and one in marginal disagreement. The application of this formula results in a higher weight to the data sample in agreement, thus causing the shift of the expected value but not the broadening of the distribution.

III. INDIRECT CONSTRAINTS FROM DISTANCE MEASUREMENTS

As discussed in [5], indirect constraints on the evolution $T(z)$, which are complementary (and competitive) to the direct bounds discussed above, can be obtained from the comparison between different distance measurements at the same redshift. In the standard cosmological picture, photon number is conserved and so luminosity distances should agree with other distance measures, as for example

angular diameter or radial $H(z)$ distance determinations. However, if photon number conservation is fundamentally—or effectively—violated, there will be a systematic mismatch between luminosity distances that depend crucially on conservation of photon number, and other distance measures that are not sensitive to photon number conservation.

Any deviation from the standard picture in which photons can decay or be absorbed or emitted along the line of sight would give rise to such a breakdown of “distance duality” [30]. Examples include couplings of photons with axions and axionlike scalar fields [31,32], or other particles beyond the standard model (see [33] and references therein), phenomenological models of dark energy interacting with photons [34,35], a hypothetical grey dust [36], or intergalactic dust [37]. Note that in the case of couplings between axionlike scalars and photons, the overall effect can also lead to an apparent brightening of the source, for example, if axions are also emitted at the source and subsequently decay to photons along the line of sight.

The potential mismatch between different distance determinations due to any of the above effects can be readily constrained at the percent level with current data.

Traditionally this has been done by constraining possible violations of the so-called Etherington (or distance duality) relation [38] through the parametrization:

$$d_L(z) = d_A(z)(1+z)^{2+\epsilon}. \quad (2)$$

Here, ϵ simply parametrizes deviations from the standard relation between luminosity distance d_L and angular diameter distance d_A . This parametrization is not physically motivated but it is adequate at low redshifts $z \lesssim 1$ for which $\epsilon z \ll 1$, thus matching the first term in a Taylor expansion, proportional to ϵz . As more data at larger redshifts are now becoming available, a more appropriate parametrization is required. When particular physical models are considered, for example SN dimming or brightening due to couplings of photons with axions or other particles beyond the standard model, specific parametrizations can be used [33], guided by the physics of each model. However, generic bounds are usually quoted in terms of the parameter ϵ .

If such a violation of the distance duality relation was due to fundamental interactions between optical photons from supernovae and some other field permeating space, one would expect that the same field would also interact with CMB photons, causing for example spectral distortions [39] (see also [40,41]). In Ref. [5], the authors pointed out that since these couplings could also cause deviations from the standard temperature evolution law discussed above (1), constraints in the parameters ϵ in (2) and β in (1) should be explicitly related within a given model. In particular, for the simplest possible case of adiabatic achromatic dimming of the CMB, the relation between β and ϵ is

$$\beta = -\frac{2}{3}\epsilon. \quad (3)$$

Further, in [35], these potential deviations from the standard $T(z)$ law and the distance duality relation were linked to variations of constants of nature, in particular the fine structure constant α . Assuming that the α variation is due to a linear gauge kinetic function (a well-motivated scenario, as discussed in [42]) and further using adiabatic achromatic dimming as a toy example, one finds a simple linear relation between ϵ , β and $\Delta\alpha/\alpha$. Such relations are, of course, model dependent and can be more complicated in realistic models. In [43], the authors did this calculation for generic non-minimal multiplicative couplings between a scalar field and the matter sector, which produce nonadiabatic dimming. This confirms the simple linear relation between β and $\Delta\alpha/\alpha$ to lowest order, correcting the relevant coefficient by a factor of order unity: the coefficient $-2/3$ in Eq. (3) would change to -0.24 . Therefore, using the adiabatic approximation actually yields a more conservative indirect bound on β from distance duality tests.

These parametric relations among violations of standard physical laws (that can be probed with different observables) provide an important tool for bootstrapping

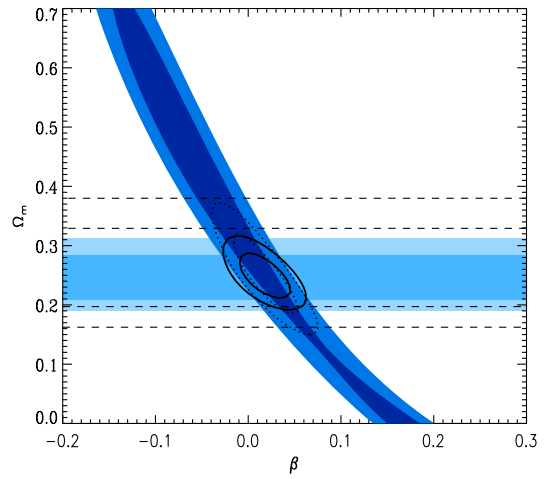


FIG. 2. Constraints from SN + $H(z)$ on the parameter β , parametrizing violations of the temperature-redshift relation as $T(z) = T_0(1+z)^{1-\beta}$. Dark blue contours correspond to 68% and 95% confidence levels obtained from SN data alone, light blue contours are for $H(z)$ data, and solid line transparent contours show the joint SN + $H(z)$ constraint. There is significant improvement from the previous constraint of Ref. [5] (dotted contours), which comes mainly from the inclusion of more $H(z)$ /BAO data points compared to the “cosmic chronometer” determinations [45] (dashed lines) used in [5].

observational constraints on the cosmological paradigm. Thus, spectroscopic and SZ determinations of $T(z)$, SN luminosity distances, BAO and $H(z)$ data from galaxy aging can be optimally combined to cross-check constraints and break degeneracies. They provide an exciting opportunity to probe fundamental high-energy physics interactions like scalar-photon couplings suppressed by energy scales of order $\sim 10^{10}$ GeV, using low-energy observations of \sim eV scale photons in the late Universe.

We first update previous indirect constraints on β using the latest available distance determinations. We use the SDSS-II/SNLS3 JLA sample [44] for luminosity distances and compare with a number of different determinations of $H(z)$: cosmic chronometers [45–47] (11 data points in the redshift range $0.1 < z < 1.75$) and the more recent [48] (8 data points at $0.17 < z < 1.1$), BAO combined with Alcock-Paczynski (AP) distortions to separate the radial component in the WiggleZ Dark Energy Survey [49] (3 data points at $z = 0.44, 0.6$ and 0.73), the SDSS DR7 BAO measurement [50] at $z = 0.35$, the BOSS DR11 measurement [51] at $z = 0.57$, and the recent $H(z)$ determination at $z = 2.3$ from BAO in the Ly α forest of BOSS DR11 quasars [52]. This gives 25 data points in the range $0.1 < z < 2.3$.

Figure 2 shows our joint constraint on the $\beta - \Omega_m$ plane. We have taken flat Λ CDM models, marginalized over H_0 , and have assumed the simple relation (3) between β and ϵ in (1) and (2), respectively. Marginalizing over Ω_m gives

$$\beta = 0.020 \pm 0.018(1\sigma), \quad (4)$$

which is competitive to the most stringent constraints from the direct probes of Sec. II and is subject to completely different systematics. Note that the constraint on the matter density coming from $H(z)$, namely $\Omega_m = 0.244^{+0.039}_{-0.034}$ (light blue horizontal contours), is consistent with the more stringent Planck result $\Omega_m = 0.308 \pm 0.012$ [1] at 95% confidence. We have not included this as an additional prior in our analysis, as here we are interested in constraining β from data sets at much lower redshifts. In particular, Fig. 2 focuses on the constraint on β coming from current distance measurement data. As we will see in the next section, the combination of this constraint (4) with direct bounds on β yields the first subpercent constraints on the cosmic temperature-redshift evolution.

IV. DATA COMBINATION AND DISCUSSION

The combination of direct and indirect bounds on the parameter β discussed in Secs. II and III above leads to a significant improvement of the overall constraint on β with an uncertainty on the temperature growth index reaching down to subpercent levels. In Table III, we show the joint constraints corresponding to Table II but now also including the indirect constraint coming from distance measurements. The PDF of this indirect constraint is represented by the green dashed lines in Fig. 1, while the final joint PDFs resulting from the combination of direct and indirect measurements are depicted by the green solid lines.

Two comments are in order regarding the interpretation and model dependence of these results. Direct determinations of $T(z)$ are subject to systematic uncertainties which have been included in the errors we have used in our analysis. On the other hand, the link between distance measurement constraints and bounds on deviations from the temperature-redshift relation is model dependent. In particular, when connecting constraints coming from

supernovae observations (optical photons) to deviations of the CMB temperature from its standard form (probed at much longer wavelengths), one implicitly assumes that the dimming mechanism is wavelength independent. This is a strong assumption, but a plausible one over a wide range of photon frequencies, for example in the context of axion-photon couplings. Further, on general grounds, couplings of this type are expected to be weaker for lower photon frequencies so assuming a frequency-independent coupling as we did yields conservative bounds on $T(z)$ violations from SN data.

The parametrizations we have used in (1) and (2) to quantify deviations from the standard temperature-redshift and luminosity-angular diameter distance relationships are standard in the literature, so constraints are better expressed in terms of these parameters to facilitate direct comparisons with other bounds in the literature (refer to Secs. II and III). However, they are phenomenological and are not directly derived from any particular theoretical model. Since deviations from the standard relations are constrained to be small, and are currently mostly probed down to redshifts of order unity, these parametrizations are adequate at present. In particular, Taylor-expanding equations (1) and (2) in redshift allows comparison to physical variables in any given model. As more data at larger redshifts are gradually becoming available, the lowest-order Taylor approximation breaks down (at $z > \text{few}$) and more accurate parametrizations are needed. This can be done in a model-to-model basis. For example, in the case of SN dimming or brightening due to couplings of photons with axions or other particles beyond the standard model, specific parametrizations can be used [33], which are guided by the physics of each model. The simple parametrizations used in this work remain useful as a phenomenological way to study deviations from the standard $T(z)$ and distance duality relationships, without referring to a specific physical model.

V. CONCLUSIONS

We have revisited existing constraints on deviations from the adiabatic evolution of the CMB black-body temperature, and by combining the latest direct (thermal SZ effect and precision spectroscopy) and indirect (distance measures) probes, we obtained the first subpercent constraint on such deviations, parametrized by the simple phenomenological law given by Eq. (1). Namely, we have found $\beta = (7.6 \pm 8.0) \times 10^{-3}$ at the 68.3% confidence level (Table III). These measurements provide an important consistency test of the standard cosmological model (as any deviation from adiabaticity will imply the presence of new physics) and also provide an important external data set for other cosmological probes such as Euclid [35].

We note that although Eq. (1) is a reasonable parametrization at low redshifts (specifically, for $z \lesssim 1$), it is not expected to be realistic for larger redshift ranges, in the

TABLE III. Joint constraints on the β parameter, derived through the combination of different constraints shown in Table I and the indirect constraints of Sec. III. The first column indicates the specific combination, represented by the labels listed in the last column of Table I. The label [indirect] corresponds to the constraint (4) of Sec. III. Individual and joint probability density functions are also plotted in Fig. 1.

| Combination | β |
|---|-----------------------|
| $[b] + [c] + [f] + [l] + [i] + [\text{indirect}]$ | 0.0076 ± 0.0080^a |
| $[a] + [e] + [l] + [h] + [\text{indirect}]$ | 0.0147 ± 0.0099 |
| $[a] + [j] + [l] + [\text{indirect}]$ | 0.013 ± 0.010^b |
| $[c] + [k] + [l] + [\text{indirect}]$ | 0.0014 ± 0.0087 |

^aApplying the prescription of [29], we get 0.0106 ± 0.0076 .

^bIn this case, there are 16 overlapping clusters between the SPT sample from [18] and the Planck sample from [17]. If we use the value given in [18], in which they removed the 16 SPT clusters that were part of the main sample analyzed by Hurier *et al.* (2014), we have $\beta = 0.010 \pm 0.010$. However, in this last case, there are 13 overlapping clusters between [17] and [14].

sense that physically motivated models will typically lead to a different behavior in the matter era. We have used it in the present work for the simple reason that it is the canonical one in the currently available literature, and therefore it allows the results of our analysis to be easily compared with those of earlier works. Nevertheless, it is already clear that as the quality, quantity, and redshift span of the data improve, more realistic classes of models should be tested.

Very significant improvements are expected in the coming years. The next generation of space-based CMB missions (e.g., a CORE/PRISM-like mission [53]) may improve the number of available SZ measurements of the CMB temperature by as much as 2 orders of magnitude, although detailed simulations of the impact of such a data set remain to be done. As for spectroscopic measurements, ALMA and ESPRESSO will soon be making significant contributions [54–56], and the prospects are even better for the high-resolution ultrastable spectrograph at the European Extremely Large Telescope [57]. In this case, most of the

progress is expected to come from CO measurements which are signal-to-noise limited. (CN would provide an even better thermometer, but so far this has not been detected in high-redshift absorption systems [58].) A road map for these measurements and a discussion of their role in precision consistency tests of the standard model can be found in [59].

ACKNOWLEDGMENTS

This work was supported by Fundação para a Ciência e a Tecnologia (FCT) through the Research Grants No. PTDC/FIS/111725/2009 and No. UID/FIS/04434/2013. C. J. M. is also supported by an FCT Research Professorship, Contract Reference No. IF/00064/2012, funded by FCT/MCTES (Portugal) and POPH/FSE (EC). A. A. is supported by the University of Nottingham Research Board through an NRF Fellowship. This work was partially supported by funding from University of Rome Sapienza 2014 C26A14FP3T. We thank A. Saro for sharing the data points plotted on Fig. 1 of [18] from the SPT analysis.

-
- [1] P. A. R. Ade, N. Aghanim, M. Arnaud, M. Ashdown, J. Aumont, C. Baccigalupi, A. J. Banday, R. B. Barreiro, J. G. Bartlett *et al.* (Planck Collaboration), [arXiv:1502.01589](https://arxiv.org/abs/1502.01589).
 - [2] L. Anderson *et al.*, *Mon. Not. R. Astron. Soc.* **441**, 24 (2014).
 - [3] A. G. Riess *et al.* (Supernova Search Team), *Astron. J.* **116**, 1009 (1998).
 - [4] S. Perlmutter *et al.*, *Astrophys. J.* **517**, 565 (1999).
 - [5] A. Avgoustidis, G. Luzzi, C. J. A. P. Martins, and A. M. R. V. L. Monteiro, *J. Cosmol. Astropart. Phys.* **02** (2012) 013.
 - [6] J. Chluba, *Mon. Not. R. Astron. Soc.* **443**, 1881 (2014).
 - [7] J. A. S. Lima, A. I. Silva, and S. M. Viegas, *Mon. Not. R. Astron. Soc.* **312**, 747 (2000).
 - [8] D. J. Fixsen, *Astrophys. J.* **707**, 916 (2009).
 - [9] R. Fabbri, F. Melchiorri, and V. Natale, *Astrophys. Space Sci.* **59**, 223 (1978).
 - [10] Y. Rephaeli, *Astrophys. J.* **241**, 858 (1980).
 - [11] R. A. Sunyaev and Y. B. Zeldovich, *Astrophys. Space Sci.* **7**, 3 (1970).
 - [12] I. de Martino, F. Atrio-Barandela, A. da Silva, H. Ebeling, A. Kashlinsky, D. Kocevski, and C. J. A. P. Martins, *Astrophys. J.* **757**, 144 (2012).
 - [13] E. S. Battistelli, M. De Petris, L. Lamagna, F. Melchiorri, E. Palladino, G. Savini, A. Cooray, A. Melchiorri, Y. Rephaeli, and M. Shimon, *Astrophys. J. Lett.* **580**, L101 (2002).
 - [14] G. Luzzi, M. Shimon, L. Lamagna, Y. Rephaeli, M. De Petris, A. Conte, S. De Gregori, and E. S. Battistelli, *Astrophys. J.* **705**, 1122 (2009).
 - [15] I. de Martino, R. Génova-Santos, F. Atrio-Barandela, H. Ebeling, A. Kashlinsky, D. Kocevski, and C. J. A. P. Martins, *Astrophys. J.* **808**, 128 (2015).
 - [16] G. Luzzi, R. T. Génova-Santos, C. J. A. P. Martins, M. De Petris, and L. Lamagna, *J. Cosmol. Astropart. Phys.* **09** (2015) 011.
 - [17] G. Hurier, N. Aghanim, M. Douspis, and E. Pointecouteau, *Astron. Astrophys.* **561**, A143 (2014).
 - [18] A. Saro *et al.* (SPT Collaboration), *Mon. Not. R. Astron. Soc.* **440**, 2610 (2014).
 - [19] S. Muller, A. Beelen, J. H. Black, S. J. Curran, C. Horellou, S. Aalto, F. Combes, M. Guélin, and C. Henkel, *Astron. Astrophys.* **551**, A109 (2013).
 - [20] P. Noterdaeme, P. Petitjean, R. Srianand, C. Ledoux, and S. López, *Astron. Astrophys.* **526**, L7 (2011).
 - [21] J. Cui, J. Bechtold, J. Ge, and D. M. Meyer, *Astrophys. J.* **633**, 649 (2005).
 - [22] J. Ge, J. Bechtold, and V. P. Kulkarni, *Astrophys. J. Lett.* **547**, L1 (2001).
 - [23] R. Srianand, P. Petitjean, and C. Ledoux, *Nature (London)* **408**, 931 (2000).
 - [24] R. Srianand, P. Noterdaeme, C. Ledoux, and P. Petitjean, *Astron. Astrophys.* **482**, L39 (2008).
 - [25] P. Noterdaeme, P. Petitjean, C. Ledoux, S. López, R. Srianand, and S. D. Vergani, *Astron. Astrophys.* **523**, A80 (2010).
 - [26] P. Molaro, S. A. Levshakov, M. Dessauges-Zavadsky, and S. D’Odorico, *Astron. Astrophys.* **381**, L64 (2002).
 - [27] J. N. Bahcall and R. A. Wolf, *Astrophys. J.* **152**, 701 (1968).
 - [28] P. A. R. Ade, N. Aghanim, M. Arnaud, M. Ashdown, J. Aumont, C. Baccigalupi, A. J. Banday, R. B. Barreiro, R. Barrena *et al.* (Planck Collaboration), [arXiv:1502.01598](https://arxiv.org/abs/1502.01598).
 - [29] G. D’Agostini, [arXiv:hep-ex/9910036](https://arxiv.org/abs/hep-ex/9910036).
 - [30] B. A. Bassett and M. Kunz, *Phys. Rev. D* **69**, 101305 (2004).

- [31] C. Csaki, N. Kaloper, and J. Terning, *Phys. Rev. Lett.* **88**, 161302 (2002).
- [32] C. Csaki, N. Kaloper, and J. Terning, *Phys. Lett. B* **535**, 33 (2002).
- [33] A. Avgoustidis, C. Burrage, J. Redondo, L. Verde, and R. Jimenez, *J. Cosmol. Astropart. Phys.* **10** (2010) 024.
- [34] C. Burrage, *Phys. Rev. D* **77**, 043009 (2008).
- [35] A. Avgoustidis, C. J. A. P. Martins, A. Monteiro, P. Vielzeuf, and G. Luzzi, *J. Cosmol. Astropart. Phys.* **06** (2014) 062.
- [36] A. N. Aguirre, *Astrophys. J.* **512**, L19 (1999).
- [37] B. Menard, M. Kilbinger, and R. Scranton, *Mon. Not. R. Astron. Soc.* **406**, 1815 (2010).
- [38] J. M. H. Etherington, *Philos. Mag.* **15**, 761 (1933).
- [39] A. Mirizzi, G. G. Raffelt, and P. D. Serpico, *Phys. Rev. D* **72**, 023501 (2005).
- [40] G. F. R. Ellis, R. Poltis, J.-P. Uzan, and A. Weltman, *Phys. Rev. D* **87**, 103530 (2013).
- [41] P. Brax, C. Burrage, A.-C. Davis, and G. Gubitosi, *J. Cosmol. Astropart. Phys.* **11** (2013) 001.
- [42] G. Dvali and M. Zaldarriaga, *Phys. Rev. Lett.* **88**, 091303 (2002).
- [43] A. Hees, O. Minazzoli, and J. Larena, *Phys. Rev. D* **90**, 124064 (2014).
- [44] M. Betoule *et al.* (SDSS Collaboration), *Astron. Astrophys.* **568**, A22 (2014).
- [45] D. Stern, R. Jimenez, L. Verde, M. Kamionkowski, and S. A. Stanford, *J. Cosmol. Astropart. Phys.* **02** (2010) 008.
- [46] J. Simon, L. Verde, and R. Jimenez, *Phys. Rev. D* **71**, 123001 (2005).
- [47] R. Jimenez, L. Verde, T. Treu, and D. Stern, *Astrophys. J.* **593**, 622 (2003).
- [48] M. Moresco, A. Cimatti, R. Jimenez, L. Pozzetti, G. Zamorani *et al.*, *J. Cosmol. Astropart. Phys.* **08** (2012) 006.
- [49] C. Blake, S. Brough, M. Colless, C. Contreras, W. Couch *et al.*, *Mon. Not. R. Astron. Soc.* **425**, 405 (2012).
- [50] X. Xu, A. J. Cuesta, N. Padmanabhan, D. J. Eisenstein, and C. K. McBride, *Mon. Not. R. Astron. Soc.* **431**, 2834 (2013).
- [51] L. Anderson *et al.* (BOSS Collaboration), *Mon. Not. R. Astron. Soc.* **441**, 24 (2014).
- [52] T. Delubac *et al.* (BOSS Collaboration), *Astron. Astrophys.* **574**, A59 (2015).
- [53] P. André *et al.* (PRISM Collaboration), *J. Cosmol. Astropart. Phys.* **02** (2014) 006.
- [54] V. Fish, W. Alef, J. Anderson, K. Asada, A. Baudry *et al.*, [arXiv:1309.3519](https://arxiv.org/abs/1309.3519).
- [55] R. Tilanus, T. Krichbaum, J. Zensus, A. Baudry, M. Bremer *et al.*, [arXiv:1406.4650](https://arxiv.org/abs/1406.4650).
- [56] F. Pepe *et al.*, *The Messenger* **153**, 6 (2013).
- [57] J. Liske *et al.*, Top Level Requirements For ELT-HIRES, Document No. ESO 204697 Version 1 (2014).
- [58] J. Krelowski, G. Galazutdinov, and P. Gnaciński, *Astron. Nachr.* **333**, 627 (2012).
- [59] C. J. A. P. Martins, *Gen. Relativ. Gravit.* **47**, 1843 (2015).